pH-Sensitive branched β-glucan-modified liposomes for activation of antigen presenting cells and induction of antitumor immunity

doi: https://doi.org/10.1039/D1TB00786F

pH-Sensitive branched β-glucan-modified liposomes for activation of antigen presenting cells and induction of antitumor immunity

Shin Yanagihara, Nozomi Kasho, Koichi Sasaki, Naoto Shironaka, Yukiya Kitayama, Eiji Yuba*, Atsushi Harada*

Department of Applied Chemistry, Graduate School of Engineering, Osaka Prefecture University, 1–1 Gakuen–cho, Naka–ku, Sakai, Osaka 5998531, Japan

*Correspondence: yuba@chem.osakafu-u.ac.jp and harada@chem.osakafu-u.ac.jp

Tel.: +81-72-254-9330; Fax: +81-72-254-9330

Abstract

Induction of cellular immunity is important for effective cancer immunotherapy. Although various antigen carriers for cancer immunotherapy have been developed to date, balancing efficient antigen delivery to antigen presenting cells (APCs) and their activation via innate immune receptors, both of which are crucially important for induction of strong cellular immunity, remains challenging. For this study, branched β-glucan was selected as an intrinsically immunity-stimulating and biocompatible material. It was engineered to develop multifunctional liposomal cancer vaccines capable of efficient interactions with APCs and subsequent activation of the cells. Hydroxy groups of branched β-glucan (Aquaβ) were modified with 3-methylglutaric acid ester and decyl groups, respectively, to provide pH-sensitivity and anchoring capability to liposomal membrane. Modification efficiency of Aquaβ derivatives to the liposomes was significantly high compared with linear β-glucan (curdlan) derivatives. Aquaβ derivative-modified liposomes released their contents in response to weakly acidic pH. As a model antigenic protein, ovalbumin (OVA)-loaded liposomes modified with Aquaβ derivatives interacted efficiently with dendritic cells, and induced inflammatory cytokine secretion from the cells. Subcutaneous administration of Aquaβ derivative-modified liposomes suppressed the growth of E.G7-OVA tumor significantly

compared with curdlan derivative-modified liposomes. Aquaβ derivative-modified liposomes induced the increase of $CD8^+$ T cells, and polarized macrophages to antitumor M1-phenotype within the tumor microenvironment. Therefore, pH-sensitive Aquaβ derivatives can be promising materials for liposomal antigen delivery systems to induce antitumor immune responses efficiently.

Keywords: liposome; polysaccharide; β-glucan; dendritic cell; cellular immunity; tumor microenvironment

1. Introduction

Cancer immunotherapy has gained much attention as a promising therapeutic approach for cancers since the success of immune checkpoint inhibitors [1]. To obtain therapeutic effects against cancer, the induction and activation of cell-based immunity (cellular immunity) are crucially important because cytotoxic T lymphocytes (CTLs) attack antigen-expressing tumor cells directly and specifically [2,3]. However, cancer-specific CTLs are not induced effectively in most patients. In addition, the CTL activity is suppressed under immunosuppressive microenvironments of tumor tissues [4]. Therefore, engineering approaches are desired to control the immune responses artificially for induction of cellular immunity and to cancel immunosuppressive environments within tumors.

To induce cancer-specific cellular immunity, exogenous antigens should be presented onto major histocompatibility complex (MHC) class-I molecules of antigen presenting cells (APCs) in a process designated as “cross-presentation” [5-7]. For induction of cross-presentation, the control of antigen delivery processes, such as antigen uptake by endocytosis through specific receptors expressed on APCs (such as mannose receptors) and cytosolic transport of antigen, is extremely important [5-8]. Cytosolic release of antigens can be achieved by mimicking viral entry into cells using

55 membrane fusion with plasma membrane or endosomal membrane [9,10]. To date,
56 various virus-derived fusogenic protein-based or synthetic molecule-based membrane
57 fusion systems have been developed to achieve efficient cytosolic delivery of antigens
58 [9,10].

59 In addition to the control of antigenic intracellular pathways, activation of innate
60 immune pathways is crucially important to induce antigen-specific cellular immunity.
61 For example, when pathogens invade the body, dendritic cells (DCs) are activated *via*
62 pattern recognition receptors such as toll-like receptors (TLRs) to induce adaptive
63 immunity against pathogens effectively [11-15]. Importantly, activated DCs decrease
64 the uptake capability of antigens [16,17]. Therefore, to induce antigen-specific immune
65 response effectively, it is desirable to accumulate antigen delivery functions and
66 adjuvant functions for activation of innate immunity into a single carrier. However,
67 precise control of antigen delivery processes and adjuvant functions using artificial
68 immunity-inducing system remains challenging because the intracellular fate of both
69 antigen and adjuvant molecules should be controlled accurately to achieve a cooperative
70 effect.

71 We have previously synthesized various carboxylated polyglycidols or
72 polysaccharides and modified them onto antigen-loaded liposomes to achieve cytosolic

73 release of antigens within APCs [18-21]. Carboxylated polyglycidols or polysaccharides
74 possess a hydrophobic nature after protonation of carboxy groups at acidic pH, which
75 induced destabilization of liposomal and endosomal membrane after internalization to
76 the cells, leading to cytosolic delivery of the antigen [18-21]. In addition, carboxylated
77 polyglycidols with a hyperbranched structure were found to have enhanced liposome
78 uptake by DCs compared with carboxylated polyglycidols having a linear structure [19].
79 This finding suggests that the bulky branched backbone structure of polymers can
80 improve interaction with immune cells. Curdlan, a linear β-glucan, is known to induce
81 activation of APCs *via* recognition by Dectin-1 on DCs and macrophages [22,23]. We
82 demonstrated that liposomes modified with 3-methylglutarylated curdlan (MGlu-Curd-
83 A, Fig. 1) can deliver model antigens into cytosol of DCs and thereby induce activation
84 of these cells [24]. After subcutaneous injection to tumor-bearing mice, ovalbumin
85 (OVA)-loaded, MGlu-Curd-A-modified liposomes induced OVA-specific cellular
86 immunity and tumor regression more effectively than OVA-loaded liposomes modified
87 with either 3-methylglutarylated dextran or mannan [24].
88 The backbone structure of carboxylated polymers dramatically affects multiple
89 aspects of liposome-based antigen delivery systems such as cellular uptake, activation
90 of innate immunity and adaptive immunity. Based on our previous observations

91 revealing that hyperbranched polyglycidol derivatives demonstrated superior

92 performance compared with their linear counterparts, here we sought to use β-glucan

93 “Aquaβ” (Fig. 1) instead of curdlan to develop a liposome-based antigen delivery

94 system with further enhanced therapeutic effects. Aquaβ has a branched structure. It is

95 known to promote secretion of inflammatory cytokines from APCs [25-27]. We

96 synthesized MGlu unit-introduced Aquaβ derivatives and evaluated the therapeutic

97 potential of Aquaβ derivative-modified liposomes containing OVA both *in vitro* and *in*

98 *vivo*. Results show that the difference in backbone structure of β-glucan increased

99 modification efficiency of polysaccharide derivatives to the liposomes and improved the

100 immunity-inducing functions considerably, especially in the infiltration of $CD8^+$ cells

101 into tumor tissue and the modulation of the macrophage composition in a tumor

102 microenvironment.

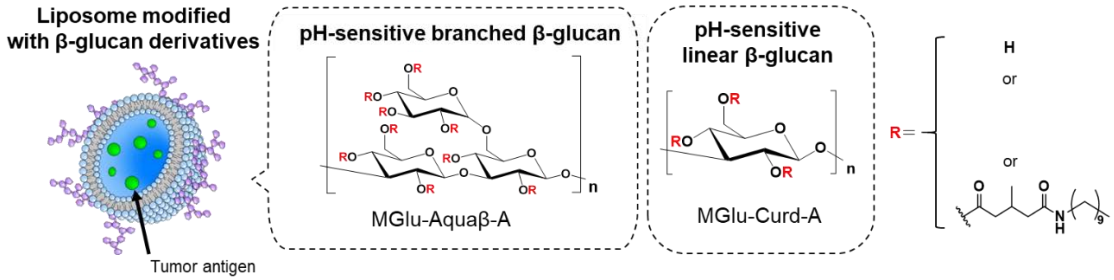

103

104 **Figure 1.** Design of antigen-loaded liposomes modified with pH-sensitive β-glucan

105 derivatives as cancer immunity-inducing systems.

2. Materials and Methods

2.1. Materials

β-1,3-1,6-glucan (Aquaβ, Mw: 100 kDa, the degree of branching is 0.71 calculated from ^{1}H NMR) was kindly donated by Osaka Soda Co., Ltd. (Osaka, Japan). Egg yolk phosphatidylcholine (EYPC) were kindly donated by NOF Co. (Tokyo, Japan). 3-Methylglutaric anhydride, curdlan from *Alcaligenes faecalis* (Mw: 294 kDa), ovalbumin (OVA), fetal bovine serum (FBS), *p*-xylene-bis-pyridinium bromide (DPX), DNase I, and dextran sulfate sodium salt from *Leuconostoc spp.* were purchased from Sigma-Aldrich (St. Louis, MO.). Collagenase D was obtained from Roche (Basel, Switzerland). 1-Aminodecane, pyranine and Triton X-100 were obtained from Tokyo Chemical Industries Ltd. (Tokyo, Japan). 4-(4,6-Dimethoxy-1,3,5-triazin-2-yl)-4-methyl morpholinium chloride (DMT-MM), phenol and phospholipid C test-Wako were from Wako Pure Chemical Industries Ltd. (Osaka, Japan). 1,1'-Dioctadecyl-3,3,3',3'-tetramethylindocarbocyanine perchlorate (DiI) was from Life Technologies (Carlsbad, CA). Fixable Viability Dye eFluor® 520 was obtained from eBioscience (San Diego, CA). Sulfuric acid and calcium chloride ($CaCl_2$) were from nacalai tesque (Kyoto, Japan). Coomassie (Bradford) Protein Assay Kit was form Thermo Fisher Scientific

K.K. (Tokyo, Japan). Sodium hydrogen carbonate was purchased from Kishida Chemical Co., Ltd. (Osaka, Japan). Cellulose tubing for dialysis (MWCO: 12,000-14,000) was obtained from Viskase Companies, Inc. (Lombard, IL).

2.2. Synthesis of β-glucan derivatives

3-Methylglutarylated Aquaβ (MGlu-Aquaβ) and 3-methylglutarylated curdlan (MGlu-Curd) were prepared by reaction of Aquaβ and curdlan with 3-methylglutaric anhydride, respectively (Fig. S1 and Table S1). A given amount of 3-methylglutaric anhydride shown in Table S1 was added to a N,N-dimethylformamide (DMF) solution of Aquaβ or curdlan and stirred at 90 ºC for 24 h under nitrogen atmosphere. Then, saturated sodium hydrogen carbonate aqueous solution was added to the reaction mixture for neutralization, and the reaction mixture was purified through a dialysis against water with dialysis membrane (MWCO: 12,000-14,000) for 3 days. The product was collected by freeze-drying. ^{1}H NMR for hydrolyzed MGlu-Aquaβ (400 MHz, D_2O + NaOD): δ 0.9 (d, J = 6.0 Hz, -CO-CH_2-CH(CH_3)-CH_2-), 2.0 (dd, J = 9.9, 14.3 Hz, -CO-CH_2-CH(CH_3)-CH_2-), 2.2-2.3 (m, -CO-CH_2-CH(CH_3)-CH_2-), 3.2-4.3 (br, glucose 2*H*, 3*H*, 4*H*, 5*H*, 6*H*), 4.5 (d, J = 7.6 Hz, β1,6-linked 1*H*), 4.7-5.1 (m, *H*DO, β1,3-linked 1*H*) [28] (Fig. S2b). ^{1}H NMR for hydrolyzed MGlu-Curd (400 MHz, D_2O + NaOD): δ

0.9 (d, J = 6.0 Hz, -CO-CH_2-CH(CH_3)-CH_2-), 2.0 (dd, J = 9.9, 14.3 Hz, -CO-CH_2-CH(CH_3)-CH_2-), 2.2-2.3 (m, -CO-CH_2-CH(CH_3)-CH_2-), 3.4-4.1 (br, glucose 2*H*, 3*H*, 4*H*, 5*H*, 6*H*), 4.7-5.1 (m, *H*DO, β1,3-linked 1*H*) [29] (Fig. S2c).

As anchor moieties for fixation of MGlu-Aquaβ and MGlu-Curd onto liposome membranes, 1-aminodecane was combined with carboxy groups of MGlu-Aquaβ and MGlu-Curd. Each polymer was dissolved in water. A given amount of 1-aminodecane shown in Table S2 was reacted with carboxy groups of the polymer using DMT-MM at room temperature for 24 h with stirring. The obtained polymers were purified through a dialysis against water with dialysis membrane (MWCO: 12,000-14,000) for more than 3 days until no water permeation within dialysis membrane takes place. The product was recovered by freeze-drying. ^{1}H NMR for hydrolyzed MGlu-Aquaβ-A (400 MHz, D_2O + NaOD): δ 0.8-1.0 (m, -CO-CH_2-CH(CH_3)-CH_2-, CO-NH-CH_2-$(CH_2)_8$-CH_3), 1.1-1.7 (br, -CO-NH-CH_2-(CH_2)$_8$-CH_3), 2.0 (dd, J = 9.9, 14.3 Hz, -CO-CH_2-CH(CH_3)-CH_2-), 2.2-2.3 (m, -CO-CH_2-CH(CH_3)-CH_2-), 3.2-4.3 (m, glucose 2*H*, 3*H*, 4*H*, 5*H*, 6*H*), 4.5 (d, J = 7.6 Hz, β1,6-linked 1*H*), 4.7-5.1 (m, *H*DO, β1,3-linked 1*H*) (Fig. S2b). ^{1}H NMR for hydrolyzed MGlu-Curd-A (400 MHz, D_2O + NaOD): δ 0.8-1.0 (m, -CO-CH_2-CH(CH_3)-CH_2-, CO-NH-CH_2-$(CH_2)_8$-CH_3), 1.1-1.7 (br, -CO-NH-CH_2-(CH_2)$_8$-CH_3), 2.0 (dd, J = 9.9, 14.3 Hz, -CO-CH_2-CH(CH_3)-CH_2-), 2.2-2.3 (m, -CO-CH_2-CH(CH_3)-CH_2-), 3.4-4.1

159 (m, glucose 2*H*, 3*H*, 4*H*, 5*H*, 6*H*), 4.5 (d, β1,6-linked 1*H*), 4.7-5.1 (m, *H*DO, β1,3-
160 linked 1*H*) (Fig. S2c).

161 2.3. Preparation of β-glucan derivative-modified liposomes

162 A given amount (5-10 mg) of EYPC dissolved in chloroform was added to round-
163 bottom flask. After evaporation of chloroform, β-glucan derivatives (lipid/polymer =
164 7/3, w/w) dissolved in methanol were added to the flask and the solvent was evaporated.
165 The remaining organic solvent was further removed under vacuum. Obtained mixed
166 thin film of EYPC and β-glucan derivatives was dispersed in phosphate-buffered saline
167 (PBS) for phenol-sulfuric acid method or OVA/PBS solution (4 mg/mL) for other
168 experiments by a brief sonication, and the liposome suspension was further hydrated by
169 freezing and thawing and was extruded through a polycarbonate membrane with a pore
170 size of 200 nm. The liposome suspension was purified with ultracentrifugation for 1 h at
171 4 °C twice.

172 2.4. Characterization of liposomes

173 Diameters and zeta potentials of the liposomes (0.1 mM of lipid concentration)
174 were measured using a Zetasizer Nano ZS (Malvern Instruments Ltd., Worcestershire,

175 UK). Data were obtained as an average of more than three measurements on different
176 samples.

177 The concentrations of lipid and OVA in liposome suspension were measured using
178 phospholipid C test-Wako and Coomassie Protein Assay Reagent, respectively.
179 Polysaccharide contents per lipid were measured by using phenol-sulfuric acid method.
180 To 200 μL aqueous solution of β-glucan derivative-modified liposomes, 200 μL of 5%
181 phenol aqueous solution and 1 mL of 98% sulfuric acid were sequentially added. The
182 mixture was vortexed and then incubated for 1 h. For a calibration curve, mixtures of 0-
183 500 μg/mL of β-glucan derivatives and EYPC suspension at an equal concentration to
184 tested β-glucan derivative-modified liposomes were prepared. Absorption spectra (400-
185 600 nm) for samples were measured and polysaccharide contents were calculated from
186 the secondary differentiation of absorbance at 497 nm.

187 Pyranine-loaded liposomes were prepared as described above except that mixture of
188 polymer and EYPC was dispersed in aqueous 35 mM pyranine, 50 mM DPX, and 25
189 mM phosphate solution (pH 7.4). Liposomes encapsulating pyranine (lipid
190 concentration: 2.0×10^{-5} M) were added to PBS of varying pH at 37 ºC and
191 fluorescence intensity at 512 nm of the mixed suspension was followed with excitation

192 at 416 nm using a spectrofluorometer (Jasco FP-6500). The release percentage of
193 pyranine from liposomes was defied as:

194 $$\text{Release}(\%) = (F_t - F_i)/(F_f - F_i) \times 100$$

195 where F_i and F_t mean the initial and intermediary fluorescence intensities of the
196 liposome suspension, respectively. F_f is the fluorescent intensity of the liposome
197 suspension after the addition of TritonX-100 (final concentration: 0.1%).

198 2.5. Cellular association of liposomes

199 DiI-labeled liposomes were prepared as described above except that a mixture of
200 polymer and lipid containing DiI (0.1 mol%) was dispersed in PBS containing OVA.
201 DC2.4 cells, a murine dendritic cell line, (7.5×10^4 cells) cultured for 2 days in a 24-
202 well plate were washed twice with HBSS and then incubated in serum-free medium
203 (0.25 mL). DiI-labeled liposomes (1 mM lipid concentration, 0.25 mL) were added
204 gently to the cells and then incubated for 4 h at 37 °C. After incubation, the cells were
205 washed with HBSS three times. Fluorescence intensity of these cells was determined *via*
206 a flow cytometric analysis (CytoFlex, Beckman Coulter, Inc.). Relative fluorescence
207 intensity for each liposome was calculated using fluorescence intensity for the cells
208 treated with unmodified liposomes. For an inhibition assay, 10 μg/mL dextran sulfate
209 was pre-incubated with cells for an hour. Then, DiI-labeled liposomes were added to the

210 cells. After 4 h incubation, fluorescence intensity of these cells was measured as
211 described above.

212 2.6. Cytokine production from dendritic cell line

213 DC2.4 cells (3×10^5 cells) cultured for 2 days in a six-well plate were washed with
214 HBSS twice and then incubated in serum-free RPMI-1640 medium. β-glucan
215 derivatives in PBS (final concentration: 0.5 mg/mL) or OVA-loaded liposomes (final
216 lipid concentration: 0.5 mM corresponding to 0.4 mg/mL lipid) were added gently to the
217 cells, followed by incubation for 24 h at 37 °C. After incubation, supernatants were
218 collected, and cytokine (IL-12 and IL-1β) production was measured using an enzyme-
219 linked immunosorbent assay kit (ELISA Development Kit, PeproTech EC Ltd.)
220 according to the manufacturer's instruction.

221 2.7. Mice

222 Seven-week-old female C57BL/6 mice ($H\text{-}2^b$) were purchased from Oriental Yeast
223 Co., Ltd (Tokyo, Japan). All animal experiments were approved by the Institutional
224 animal experimentation committee in Osaka Prefecture University (Approval No. 19-1,
225 20-1) and were performed in compliance with the institutional guidelines of animal care
226 and use.

227 2.8. Induction of antitumor immunity

228 E.G7-OVA cells, OVA-expressing T-lymphoma, (5.0×10^5 cells/mouse) were
229 subcutaneously inoculated into the left back of C57BL/6 mice under anesthesia with
230 isoflurane. On days 8 and 14, 100 μg of OVA-loaded liposomes were subcutaneously
231 injected into the right backs of the mice under anesthesia with isoflurane. Tumor sizes
232 were monitored from the day of tumor inoculation. Mice immunized with PBS were
233 used as a control to confirm the development of tumors following the first inoculation
234 of E.G7-OVA cells. Mice were sacrificed when tumor volumes became over 2,000
235 mm^3. All treated groups contained five mice.

236 2.9. Analysis of immune cell composition in the tumor

237 E.G7-OVA cells (5.0×10^5 cells/mouse) were subcutaneously inoculated into the
238 left back of C57BL/6 mice under anesthesia with isoflurane. On day 6, 100 μg of OVA-
239 loaded liposomes were subcutaneously injected into the right backs of the mice under
240 anesthesia with isoflurane. On day 12, mice were sacrificed and, tumor tissues were
241 excised. Tumor were cut into small pieces and digested by incubating in sodium
242 pyruvate-free DMEM medium supplemented with 1.2 mM $CaCl_2$, 2 mg/mL
243 Collagenase D and 0.04 mg/mL DNase I at 37 ºC for 1 h. Single cell suspension of the

tumor was prepared by gentle mashing and passing through a 70 μm mesh Cellstrainer™ (Falcon®). Erythrocytes were removed by incubating the cell pellet for 5 min in ammonium chloride buffer (7.47 mg/mL NH_4Cl, 2.06 mg/mL Tris(hydroxymethyl)aminomethane, pH 7.4) at 4 ºC. Tumor cells were seeded into 96-well plates with 1.0×10^6 cells/well and washed in PBS. To discriminate between live and dead cells, the cells were incubated for 30 min on ice with Fixable Viability Dye eFluor® 520 (diluted 1:1000 in PBS), and washed with FACS buffer (PBS containing 2% FBS) twice. The cells were incubated with 5 μg/mL CD16/CD32 monoclonal antibody (eBioscience) for 20 min at 4 ºC to block Fc receptors, and then washed twice. To analyze T cell populations, the cells were stained with anti-CD8-PE (eBioscience, 53-6.7), anti-CD3ε-PerCP-Cy5.5 (BD Bioscience, 145-2C11) and anti-CD4-PE/Cy7 (BD Bioscience, RM4-5) for 20 min at 4 ºC. For analysis of macrophage populations, the cells were stained with anti-CD206-PE (BioLegend, C068C2), anti-CD11b-PerCP-Cy5.5 (BD Pharmingen™, M1/70) and anti-I-A^b-PE/Cy7 (BioLegend, AF6-120.1) antibodies for 20 min at 4 ºC. (each diluted 1:200 in FACS buffer). After washing twice, cell populations were analyzed *via* a flow cytometric analysis.

2.10. Statistical analysis

Statistically significant differences between experimental groups were determined using Prism software (v8, GraphPad). Where one-way ANOVA followed by Tukey's HSD post hoc test was used, variance between groups was found to be similar by Brown-Forsythe test. The symbols *, **, ***, and **** indicate *P* values less than 0.05, 0.01, 0.001, and 0.0001, respectively.

3. Results

3.1. Synthesis of β-glucan derivatives and modification onto the liposomes

Synthesis of pH-sensitive Aquaβ derivatives was performed as shown in Fig. S1, and Tables S1 and S2. Hydroxy groups of Aquaβ were reacted with 3-methylglutaric anhydrides to introduce carboxylic esters (MGlu groups). Decyl groups were further introduced *via* amide bonds as an anchor moiety to fix Aquaβ derivatives onto liposomal membrane. pH-Sensitive curdlan derivatives were synthesized according to our previous report [24]. For ^{1}H NMR analysis of obtained compounds, broad peaks appeared corresponding to MGlu groups (0.9 and 1.9–2.3 ppm) and decyl groups (0.8–1.7 ppm) along with sugar moieties (3.2–4.7 ppm) (Fig. S2a), indicating the introduction of MGlu groups and decyl groups to β-glucans. The percentage of MGlu

278 groups (MGlu%) and anchor groups (anchor%) of β-glucan derivatives were calculated
279 from the peak area ratio of sugar moieties and MGlu groups or decyl groups after
280 hydrolysis by NaOD (Tables S2 and S3, Figs. S2b and S2b). The β-glucan derivatives
281 bearing various percentages of MGlu groups with comparable anchor% were
282 successfully synthesized (Tables S1 and S2). Each β-glucan derivative was designated
283 as MGluX-Curd-AY or MGluX-Aquaβ-AY, where X and Y respectively represent
284 MGlu% and anchor% per hydroxy groups. The MGlu and anchor densities per 100
285 β1,3-linked sugar units for both Aquaβ and curdlan derivatives were also calculated
286 (Table S2). The MGlu and anchor densities of Aquaβ derivatives were relatively high
287 compared with those of curdlan derivatives because of MGlu and anchor groups
288 introduced to branched sugar units of Aquaβ.

289 Using hydration of mixed thin film composed of EYPC and β-glucan derivatives,
290 the β-glucan derivatives were introduced onto liposomes. Table 1 shows the size and
291 zeta potentials of the prepared liposomes: all liposomes had 100-200 nm of average
292 size, corresponding to the pore size of polycarbonate membrane used for extrusion. It
293 was confirmed by TEM observation that the liposome structure with lipid bilayer was
294 maintained even after the modification of β-glucan derivatives (Fig. S3). Liposomes
295 prepared from the mixture of EYPC and β-glucan derivatives exhibited large absolute

296 values of negative zeta potentials compared with EYPC liposomes without polymer
297 modification, suggesting that β-glucan derivatives were modified onto liposomal
298 membranes. The amounts of β-glucan derivatives per lipid were evaluated using the
299 phenol-sulfuric acid assay, which is a standard quantitative assay of sugar [30,31]. The
300 modification efficiency of Aquaβ and curdlan derivatives were compared using β-
301 glucan derivative-modified liposomes without OVA loading (Fig. 2). It was obvious
302 that Aquaβ derivatives exhibit higher modification efficiency than curdlan derivatives,
303 and this might be due to the difference in the anchor density of β-glucan derivatives
304 (Table S2). β-glucan derivatives with relative high anchor density, i.e. Aquaβ
305 derivatives, were fixed to liposomes with high efficiency. As a model antigenic protein,
306 OVA was encapsulated into each liposome. The amounts of OVA per lipid (g/mol)
307 were 100–250 and encapsulation efficiency of OVA was 17–40%, which is comparable
308 level with our previous reports using carboxylated chondroitin sulfate derivative-
309 modified liposomes and carboxylated hyperbranched polyglycidols [21,32].

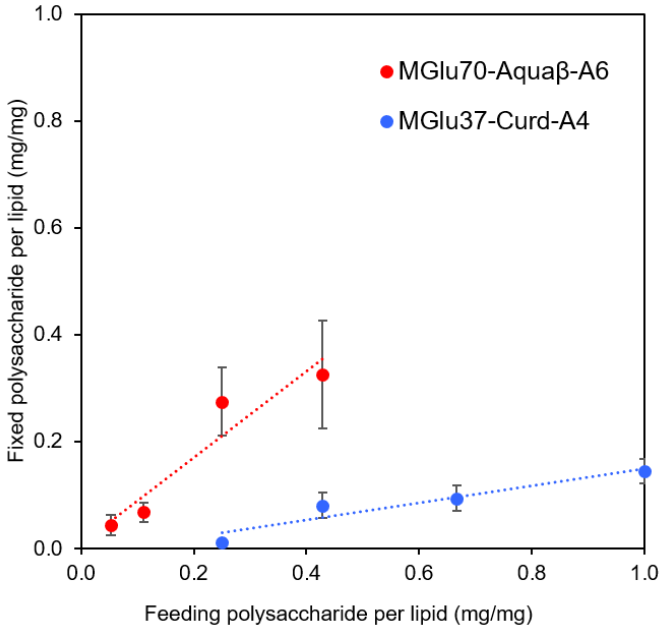

Figure 2. The modification efficiency of β-glucan derivatives to liposomes.

Correlation of modification amounts with feeding amounts of β-glucan derivatives on liposomes was shown. Modification amounts of β-glucan derivatives on liposomes were measured by the phenol-sulfuric acid method. Each point is the mean ± SD (n = 3).

Table 1. Characterization of β-Glucan Derivative-Modified Liposomes

Liposome	size (nm)	PDI	ζ-potential (mV)	OVA/lipid (g/mol)	Encapsulation efficiency (%)
Unmodified	175 ± 15	0.17 ± 0.02	-7.90 ± 2.8	253 ± 96	39.6 ± 15
MGlu70-Aquaβ-A6	126 ± 14	0.23 ± 0.04	-42.3 ± 8.0	143 ± 43	22.4 ± 6.7
MGlu56-Aquaβ-A4	119 ± 3.1	0.20 ± 0.02	-42.3 ± 5.4	116 ± 19	18.1 ± 3.0
MGlu38-Aquaβ-A3	127 ± 13	0.17 ± 0.01	-46.0 ± 10	107 ± 25	16.7 ± 3.9
MGlu21-Aquaβ-A2	148 ± 21	0.25 ± 0.06	-40.1 ± 5.0	186 ± 8.8	29.1 ± 1.4
MGlu71-Curd-A6	210 ± 32	0.16 ± 0.08	-45.3 ± 2.4	111 ± 25	17.4 ± 3.9
MGlu62-Curd-A4	139 ± 27	0.21 ± 0.01	-31.0 ± 12	204 ± 2.5	31.9 ± 0.4
MGlu37-Curd-A4	154 ± 6.6	0.14 ± 0.02	-41.1 ± 3.4	114 ± 28	17.8 ± 4.4
MGlu13-Curd-A4	103 ± 8.0	0.17 ± 0.01	-27.6 ± 6.6	118 ± 10	18.5 ± 1.6

Destabilization of Aquaβ derivative-modified liposomes in response to decrease in pH to acidic pH was evaluated using liposomes encapsulating both a fluorescent dye (pyranine) and its quencher (DPX). The increase in fluorescence intensity derived from pyranine released from the liposomes at varying pHs was monitored (Fig. 2). Although the release of pyranine from unmodified EYPC liposomes never exceeded 20% of the total amounts at any evaluated pH range, Aquaβ derivative-modified liposomes could release pyranine in response to acidic pH as same with curdlan derivative-modified liposomes (Figs. 3, S4 and S5).

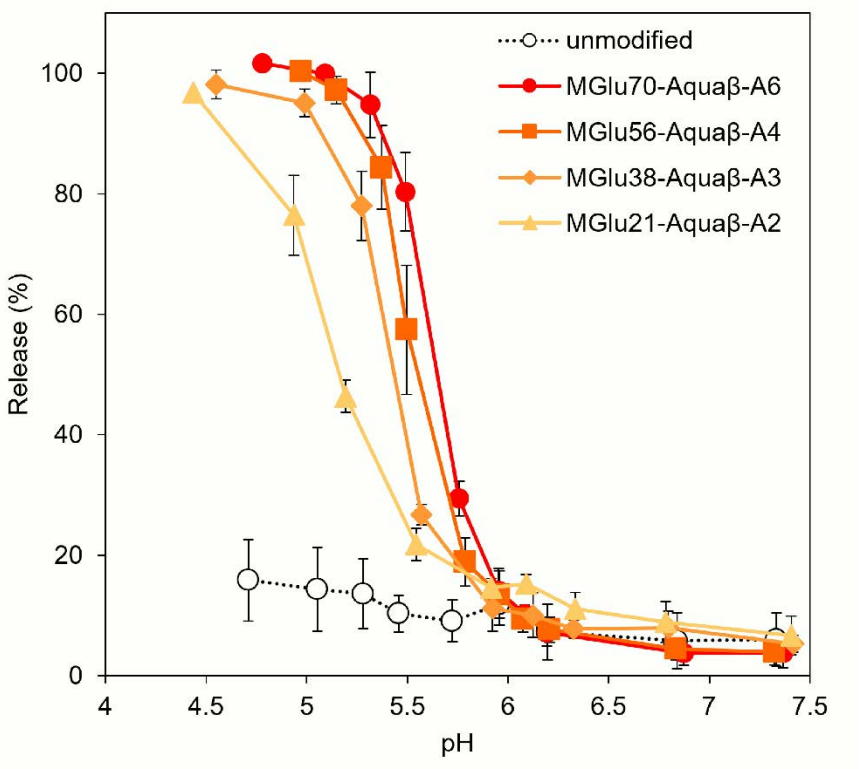

Figure 3. pH-Sensitivity of liposomes modified with Aquaβ derivatives. pH-Dependence of pyranine release from liposomes modified with or without Aquaβ derivatives after 30 min incubation are shown. Lipid concentration was 2.0×10^{-5} M. Each point is the mean ± SD (n = 3).

3.2. Adjuvant property of Aquaβ derivative-modified liposomes and their cellular interaction

Adjuvant effects of Aquaβ derivatives without modification onto liposomes were evaluated and compared with those of curdlan derivatives by measuring secretions of inflammatory cytokines from the dendritic cell line (DC2.4 cell) (Figs. 4a and 4b). After 24 h incubation of DC2.4 cells with β-glucan derivatives, inflammatory cytokines in cell culture supernatant were quantified by ELISA assay. Aquaβ with high MGlu% (MGlu63, 75) induced significantly higher amounts of IL-12 and IL-1β secretion than parental Aquaβ and Aquaβ derivatives with low MGlu%, although there was no clear correlation between cytokine production and MGlu% for curdlan derivatives. In particular, MGlu75-Aquaβ showed significantly high IL-1β secretion compared with the other β-glucan derivatives. Adjuvant effects of liposomes modified with β-glucan

derivatives were also evaluated (Figs. 4c and 4d). In both of IL-12 and IL-1β secretions, there observed significantly high secretion for liposomes modified with Aquaβ derivatives having high MGlu% compared with the other liposomes. The results suggest that liposomes modified with Aquaβ derivatives having high MGlu% activated DCs more effectively than liposomes modified with curdlan derivatives did.

The effect of feeding amounts of β-glucan derivatives to DC2.4 cells was evaluated in the amount of IL-12 secreted from the cells (Fig. 4e). Focusing on MGlu70-Aquaβ-A6 and MGlu37-Curd-A4, there observed a similar tendency to the relationship between the feeding amount and the fixed amount of β-glucan derivatives to liposomes shown in Fig. 2. However, in the comparison of β-glucan derivative-modified liposomes with similar amounts of the fixed β-glucan derivatives, Aquaβ derivative-modified liposomes promoted IL-12 secretion from DC2.4 cells more than curdlan derivative-modified liposomes did (Fig. 4e). When β-glucan derivatives-modified liposomes were prepared at the feeding of 0.11 mg / 1 mg lipid of MGlu70-Aquaβ-A6 and that of 0.43 mg / 1 mg lipid of MGlu37-Curd-A4, the obtained liposomes showed an identical fixed amount of β-glucan derivatives (Fig. 2). As these β-glucan derivatives-modified liposomes were compared, IL-12 secretion of MGlu70-Aquaβ-A6-modified liposomes showed 10 times higher than that of MGlu37-Curd-A4-modified liposomes (Fig. 4e).

Figure S6 depicts the correlation between IL-12 production and MGlu group amounts on the liposomes, which is calculated from MGlu% of each β-glucan derivative and its modification amount on the liposomes. In comparison of 0.08–0.1 mol/mol MGlu group amounts per lipid, MGlu70-Aquaβ-A6-modified liposomes showed much higher IL-12 production from the cells than MGlu37-Curd-A4- and MGlu71-Curd-A6-modified liposomes did, suggesting that high MGlu density of Aquaβ derivative-modified liposomes derived from branching structure of Aquaβ promoted the activation of DC2.4 cells. These results indicate that Aquaβ has superior DC activation capability as a backbone of carboxylated polysaccharides to curdlan.

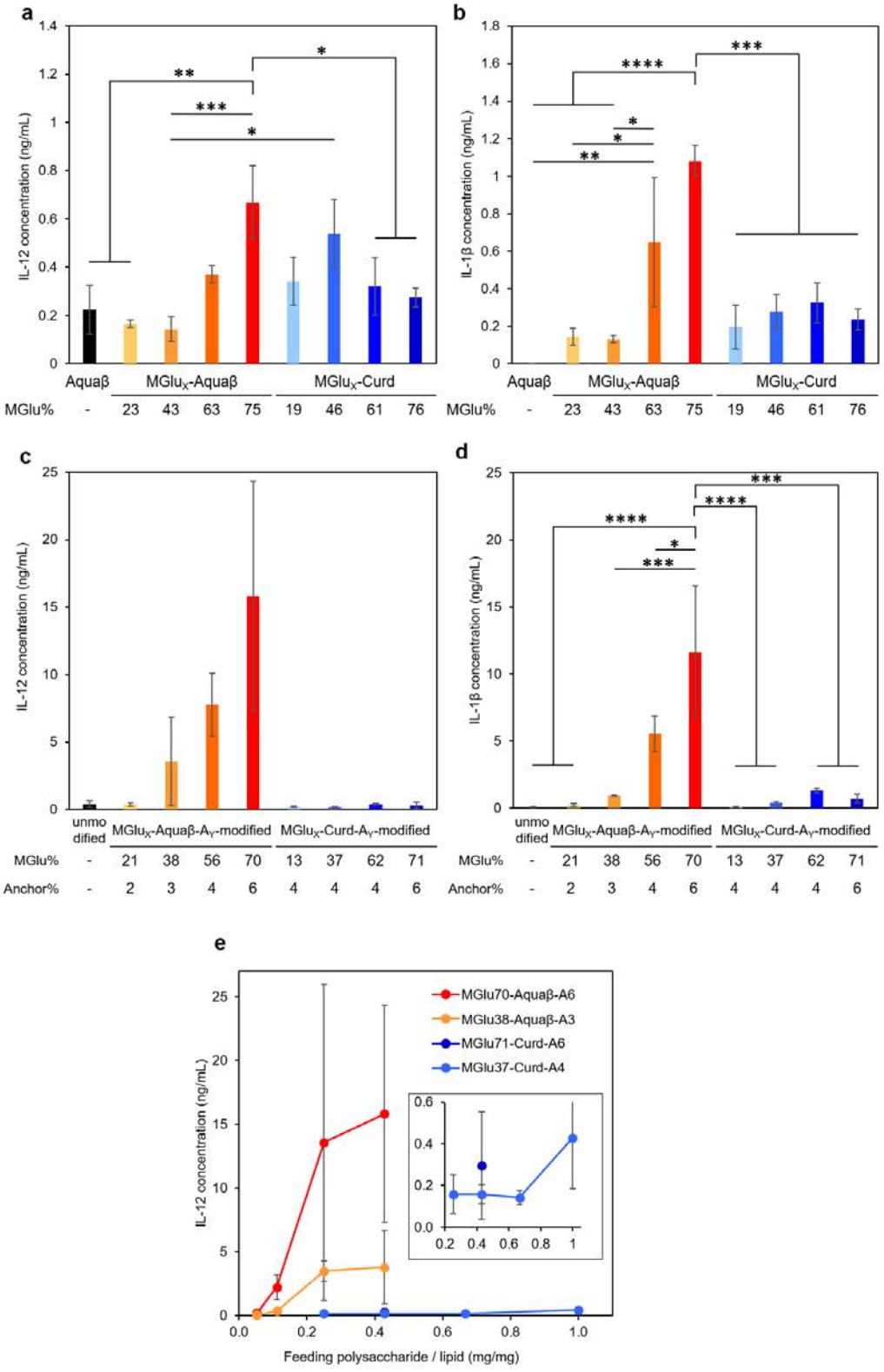
a
IL-12 concentration (ng/mL)
Aquaβ
MGlu$_X$-Aquaβ
MGlu$_X$-Curd
MGlu%
b
IL-1β concentration (ng/mL)
c
unmodified
MGlu$_X$-Aquaβ-A$_Y$-modified
MGlu$_X$-Curd-A$_Y$-modified
Anchor%
d
e
MGlu70-Aquaβ-A6
MGlu38-Aquaβ-A3
MGlu71-Curd-A6
MGlu37-Curd-A4
Feeding polysaccharide / lipid (mg/mg)

371

Figure 4. Adjuvant properties of β-glucan derivatives and β-glucan derivative-modified liposomes. Cytokine secretion from DC2.4 cells treated with (a, b) Aquaβ or β-glucan derivatives (0.5 mg/mL), or (c, d) unmodified liposomes or liposomes modified with β-glucan derivatives (0.4 mg/mL lipids) for 24 h. (e) IL-12 production from DC2.4 cells treated with β-glucan derivatives-modified liposomes that were prepared with various feeding amounts of β-glucan derivatives. Inset represents an enlarged image for the results of MGlu-Curd-A-modified liposomes. Statistical analyses were conducted using analysis of variance (ANOVA) with Tukey's test. **P*<0.05; ***P*<0.01; ****P*<0.001; *****P*<0.0001.

Interactions (association and/or uptake) of Aquaβ derivative-modified liposomes with DC2.4 cells were compared with those of curdlan derivative-modified liposomes. DC2.4 cells were treated with fluorescently labeled liposomes, and fluorescence intensity of the cells were then evaluated using flow cytometry. In the case of Aquaβ derivative-modified liposomes, all kinds of liposomes showed higher interaction than unmodified liposomes irrespective of MGlu% (Fig. 5a). On the other hand, the interaction of curdlan derivative-modified liposomes with the cells increased with an increase in MGlu% of curdlan derivatives. The interaction of liposomes with the cells in

390 the coexistence of dextran sulfate, which is known to interact with scavenger receptors
391 [33], was also evaluated in order to discuss the mechanisms of cellular interaction with
392 β-glucan derivative-modified liposomes. Although there was almost no change in
393 fluorescence intensity of the cells treated with MGlu13-Curd-A4- and MGlu37-Curd-
394 A4-modified liposomes even in the coexistence of dextran sulfate, the cellular
395 interactions of MGlu62-Curd-A4- and MGlu71-Curd-A6-modified liposomes were
396 inhibited by the presence of dextran sulfate (Fig. 5b). This result suggests that MGlu
397 units introduced into curdlan in high percentages were recognized by scavenger
398 receptors. Interestingly, the inhibitory effect of dextran sulfate on the interaction of
399 Aquaβ derivative-modified liposomes with the cells was an opposite with that of
400 curdlan derivative-modified liposomes. Dextran sulfate strongly suppressed the
401 interaction of liposomes modified with Aquaβ derivatives having low MGlu%.
402 However, the cellular interactions of Aquaβ derivatives-modified liposomes in the
403 coexistence of dextran sulfate was improved with an increase in MGlu%, and MGlu70-
404 Aquaβ-A6-modified liposomes showed the enhancement of cellular interaction by
405 dextran sulfate (Fig. 5b). These results suggest that the recognition mechanism by DCs
406 differs between curdlan derivatives- and Aquaβ derivatives-modified liposomes.

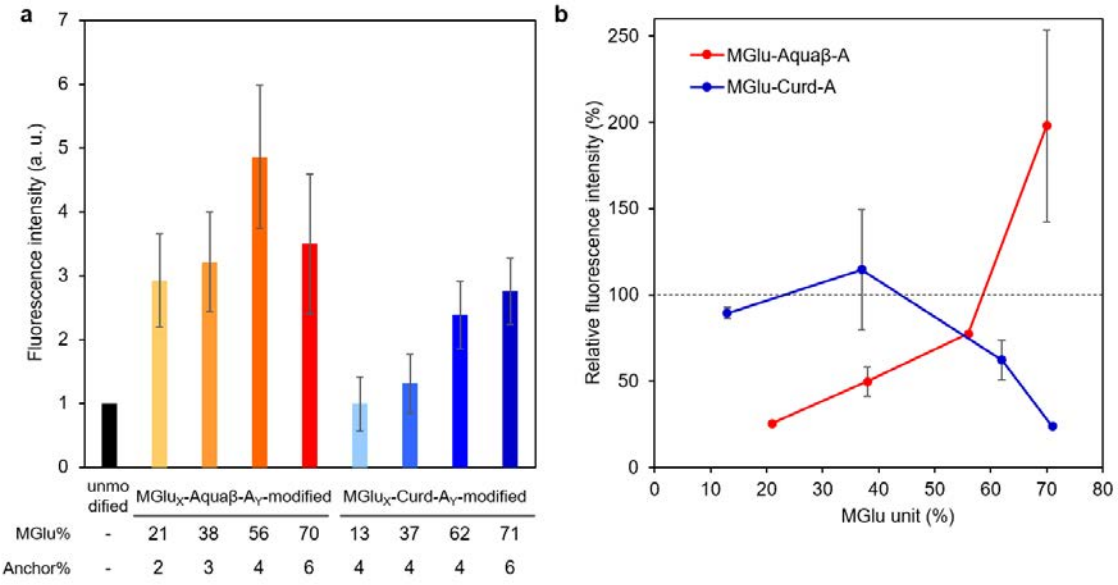

407

408 **Figure 5. Cellular association of liposomes modified with β-glucan derivatives.** (a)

409 Fluorescence intensity for DC2.4 cells treated with DiI-labeled liposomes modified with

410 or without β-glucan derivatives for 4 h. (b) DC2.4 cells were treated with DiI-labeled

411 liposomes in the presence of dextran sulfate as an inhibitor of scavenger receptors. The

412 vertical line shows the percentage of fluorescence intensity (FI) with inhibitor to FI

413 without inhibitor.

414

415 **3.3. Induction of antitumor immunity by Aquaβ derivative-modified liposomes**

416 Antitumor effects of Aquaβ derivative-modified liposomes were evaluated using

417 tumor-bearing mice. After OVA-expressing tumor cells (E.G7-OVA cells) were

418 inoculated to mice, OVA-loaded liposomes modified with β-glucan derivatives or PBS

419 were administered subcutaneously to tumor-bearing mice on Days 8 and 14 after tumor
420 inoculation. In the case of mice treated with PBS, tumor volumes increased rapidly and
421 reached endpoints within 30 days (Figs. 6 and S7). On the other hand, Aquaβ
422 derivative-modified liposomes suppressed tumor growth in all-treated mice more
423 significantly than PBS (Fig. 6 and S7). Suppression of tumor growth was not observed
424 in some mice administered with curdlan derivative-modified liposomes (Figs. 6 and S7).
425 This result suggests that Aquaβ derivative-modified liposomes have a higher therapeutic
426 effect on the E.G7-OVA cancer model than curdlan derivative-modified liposomes.
427 After the first injection of the liposomes, some mice showed a mild decrease of body
428 weight (about 5%), but they recovered quickly 2 days after the first injection (Fig. S8).
429 Decline of body weight was not observed after second injection of liposomes.
430 Therefore, toxicities of liposomes are apparently not severe. Aquaβ derivative-modified
431 liposomes did not show any cytotoxicity to the fibroblast *in vitro* (Fig. S9a), suggesting
432 that these liposomes show no remarkable cytotoxicity to the resident cells at injection
433 site. We have also investigated antigen-specific immune responses by measuring IFN-γ
434 production from splenocytes of the mice immunized with OVA-loaded liposomes. As
435 shown in Fig. S9b, no IFN-γ production was detected in the absence of *in vitro* antigen
436 (OVA) stimulation. In contrast, splenocytes of the mice immunized with Aquaβ

derivative-modified liposomes showed significant IFN-γ production in the presence of OVA stimulation. These results indicate that Aquaβ derivative-modified liposomes could induced OVA-specific cellular immune responses, which led the selective cytotoxicity against OVA-expressing tumor cells (E.G7-OVA cells) in the tumor-bearing mice.

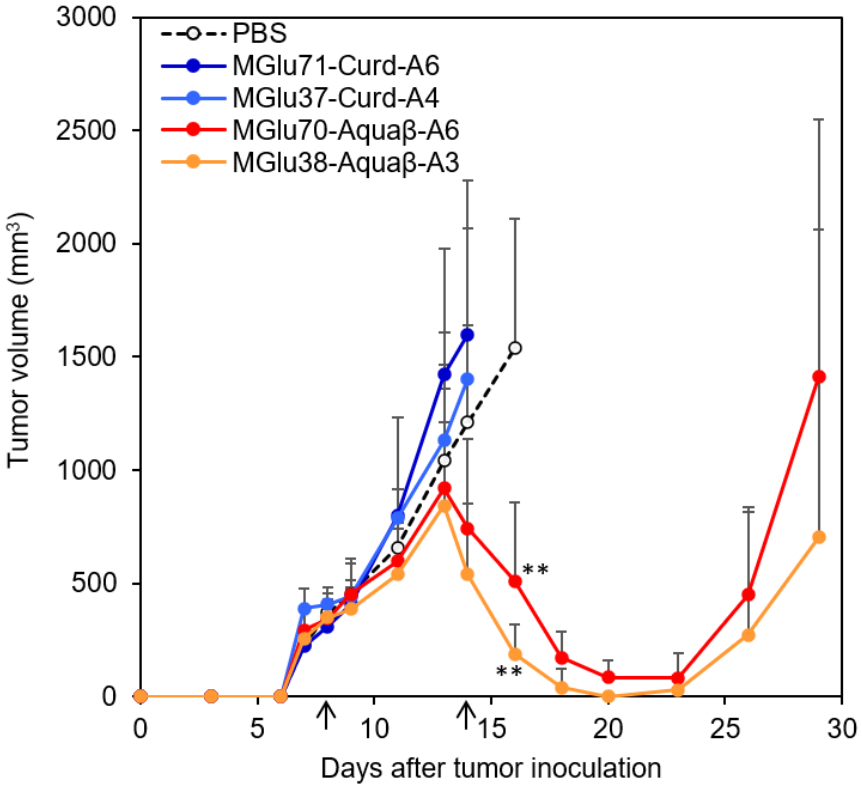

Figure 6. Antitumor effects of OVA-loaded liposomes modified with β-glucan derivatives. C57BL/6 mice were immunized on days 8 and 14 after tumor inoculation with PBS or OVA-loaded liposomes modified with β-glucan derivatives. Changes in tumor volume of mice were monitored after E.G7-OVA cells (5.0×10^5 cells/mouse)

447 inoculation. Arrows indicate the days of sample injection. All treated groups included
448 five mice. Statistical analyses comprised analysis of variance (ANOVA) with Tukey's
449 test. $^{**}P<0.01$ compared with PBS (on day 16).

450

451 **3.4. Analysis of immune cell composition after immunization of β-glucan**
452 **derivative-modified liposomes**

453 We investigated whether administration of Aquaβ derivative-modified liposomes
454 changed the composition of intratumoral immune cells, or not. Since MGlu37-Curd-A4-
455 and MGlu71-Curd-A6-modified liposomes showed almost identical antitumor effect,
456 MGlu71-Curd-A6-modified liposomes were used as a comparison for Aquaβ derivative-
457 modified liposomes. Tumors were harvested at 6 days after administration of OVA-
458 loaded liposomes modified with β-glucan derivatives to tumor-bearing mice. The
459 immune cell population in tumors was analyzed using flow cytometry. The frequency of
460 intratumoral $CD4^+$ T cell population did not change in any of the administered mice, but
461 the frequency of intratumoral $CD8^+$ T cells increased significantly in mice administered
462 with Aquaβ derivative-modified liposomes compared with PBS-administered mice (Fig.
463 7). In addition, the frequency of $CD8^+$ T cells in mice administered with MGlu38-

464 Aquaβ-A3-modified liposomes was significantly higher than that in mice administered

465 with MGlu71-Curd-A6-modified liposomes. These results indicate that Aquaβ

466 derivative-modified liposomes have excellent capability of activating cellular immunity

467 and of promoting the infiltration of CTLs into the tumor.

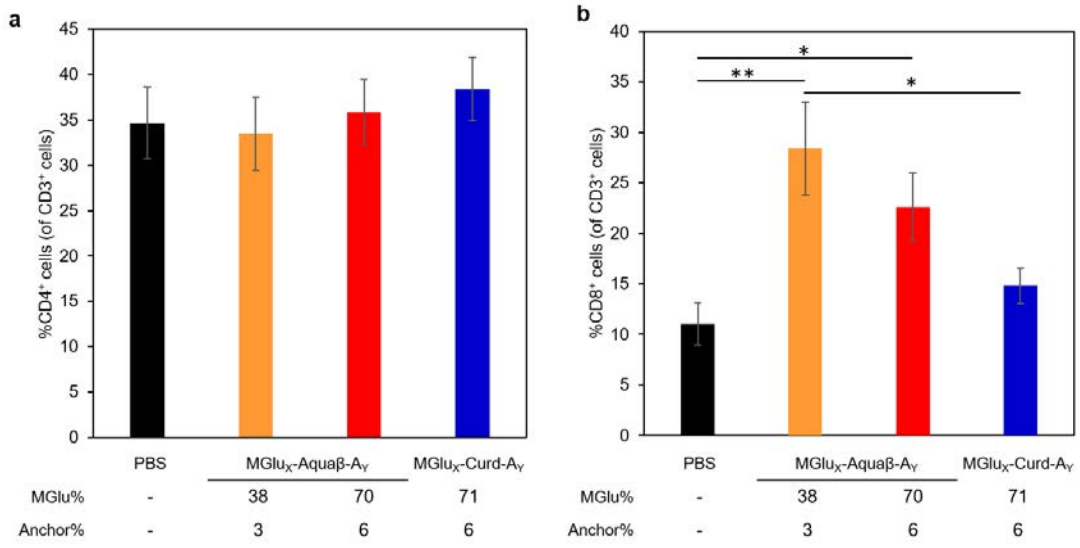

468

469 **Figure 7. T-lymphocyte analysis in a tumor.** E.G7-OVA cells were inoculated to

470 C57BL/6 mice. Then PBS or liposomes were subcutaneously immunized to these mice

471 on Day 6. Cell suspension was obtained from tumor on Day 12 followed by flow

472 cytometric analysis. Graphs depict the frequency of (a) $CD4^+$ cells within $CD3^+$ T-

473 lymphocytes and (b) $CD8^+$ cells within $CD3^+$ T-lymphocytes in live cells of tumor

474 tissue (mean ± SEM; $n = 9$ (PBS), 5 (MGlu38-Aquaβ-A3) and 10 (MGlu70-Aquaβ-A6

475 and MGlu71-Curd-A6)). Statistical analyses were done using analysis of variance

476 (ANOVA) with Tukey's test. *P<0.05; **P<0.01.

We next analyzed the intratumoral macrophage population using flow cytometry. The frequency of macrophages expressing MHC-II (M1-phenotype with antitumor character) increased only in mice treated with MGlu38-Aquaβ-A3-modified liposome (Fig. 8a). The proportion of macrophages expressing CD206 (M2-phenotype with pro-tumor character) tended to decrease more in mice treated with all β-glucan derivative-modified liposomes than in mice treated with PBS. Particularly, the percentage of intratumoral M2 macrophages in mice treated with MGlu70-Aquaβ-A6-modified liposomes was decreased significantly compared with mice treated with PBS (Fig. 8b). The ratio of M1 and M2 macrophages calculated from the results in Figs. 8a and 8b tended to be higher in Aquaβ derivative-modified liposome-administered mice than PBS-administered mice (Fig. 8c). This result was further confirmed by immunofluorescence staining of tumor section. As shown by yellow dots in Fig. S10a, administration of Aquaβ derivative-modified liposome tended to increase MHC-II$^+$ CD11b$^+$ cells within tumor tissue compared with PBS or MGlu71-Curd-A6-modified liposomes. Furthermore, administration of all β-glucan derivative-modified liposome decreased CD206$^+$ CD11b$^+$ cells within tumor tissue compared with PBS-treated groups (Fig. S10b). These results suggest that administration of Aquaβ derivative-modified

liposomes can polarize macrophages in tumors to the tumor-suppressive M1-phenotypes.

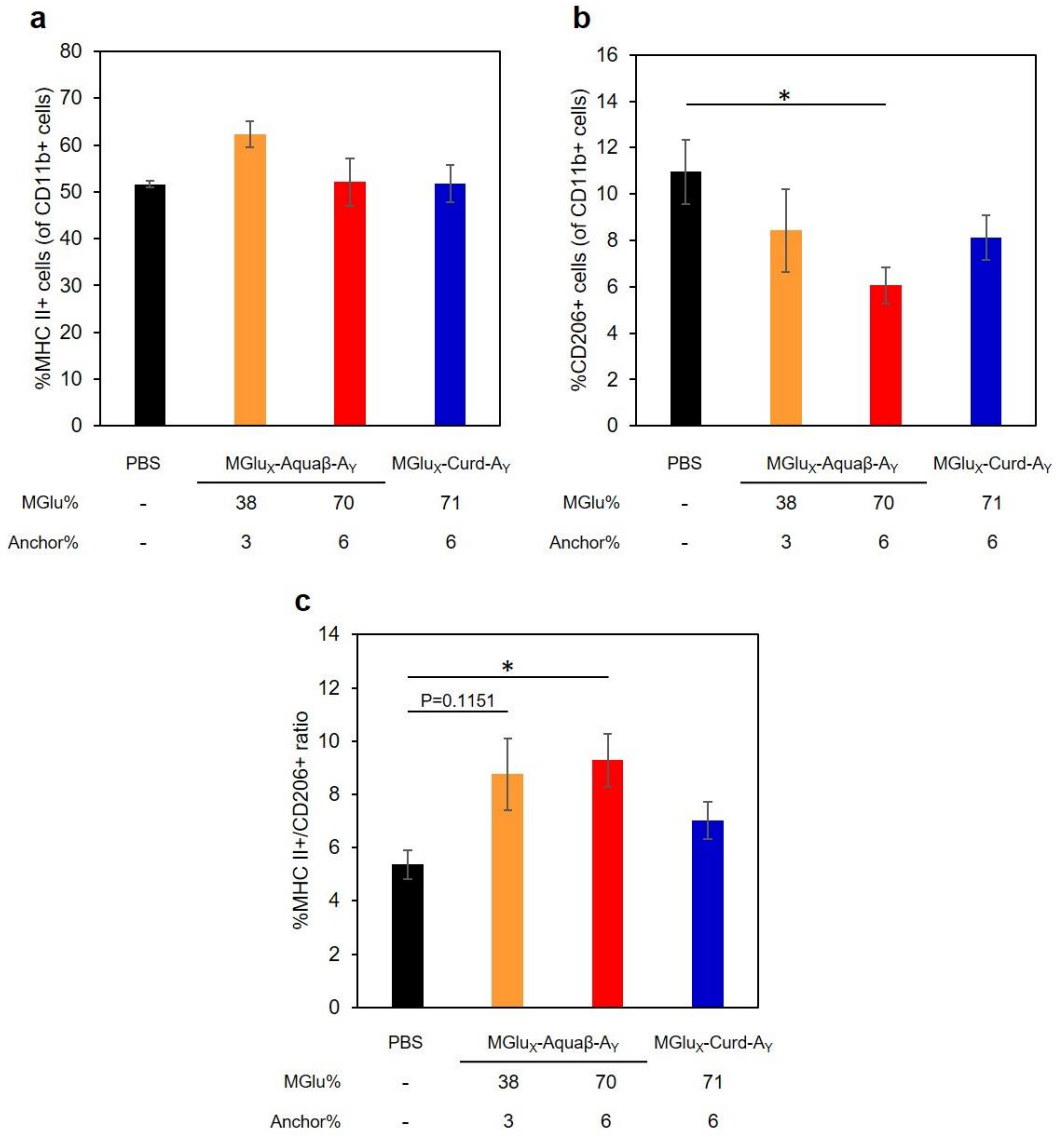

Figure 8. Macrophage analysis in a tumor. E.G7-OVA cells were inoculated to C57BL/6 mice. Then PBS or liposomes were immunized subcutaneously to the mice on Day 6. Cell suspension was obtained from tumor on Day 12, followed by flow

cytometric analysis. Graphs depict the frequency of (a) M1 macrophages (MHC II^+ $CD11b^+$), (b) M2 macrophages ($CD206^+$ $CD11b^+$) and (c) M1/M2 ratio (mean ± SEM; n = 9 (PBS), 5 (MGlu38-Aquaβ-A3) and 10 (MGlu70-Aquaβ-A6 and MGlu71-Curd-A6)). Statistical analyses were done using analysis of variance (ANOVA) with Tukey's test. *P<0.05.

4. Discussion

Activation of cancer antigen-specific CTLs, more specifically the infiltration of CTLs into tumor tissue, is important for success of immunotherapy [2,3]. To activate CTLs efficiently, promotion of cross-presentation of antigenic proteins by APC is necessary, as is activation of APC [5-7]. Cross-presentation is facilitated primarily by inducing transfer of antigenic proteins to cytosol of APCs. Antigenic proteins are degraded in cytosol and are presented on MHC-I molecules as epitope peptides [5-7]. The functional polymers having carboxylated units are protonated in response to weakly acidic pH in endosomes of APCs. The polymer then become hydrophobic, which causes membrane fusion or destabilization of liposomes and endosomal membrane. Therefore, they are often used to promote the transfer of antigenic proteins to cytosol [34,35].

518 To induce antigen-specific immune responses effectively, accumulation of an
519 adjuvant and an antigen in a single carrier, and their simultaneous delivery to APCs are
520 ideal. In our previous study, highly functional antigen carriers were developed by
521 modifying antigen-loaded liposomes with carboxylated curdlan derivatives [24]. These
522 liposomes simultaneously achieved an efficient uptake of antigenic proteins by APCs,
523 antigen release into cytosol, and activation of APCs through innate immunity pathways
524 [24].

525 In this study, we sought to improve the immunity-activation ability of liposomes by
526 changing the backbone structure of carboxylated polysaccharides from linear β-glucan
527 (curdlan) to branched β-glucan (Aquaβ). Aquaβ was derivatized using a method
528 described previously (Fig. S1). Modification of β-glucan derivatives to the liposomes
529 was confirmed by zeta potential measurement and the quantification of polysaccharide
530 contents in liposome solution (Fig. 2). Aquaβ derivative-modified liposomes exhibited
531 an identical pH-sensitive content release property with curdlan derivative-modified
532 liposomes (Figs. 3, S4 and S5). It is particularly interesting that the modification
533 efficiency of Aquaβ derivatives was much higher than that of curdlan derivatives (Fig.
534 2). This difference might be explained from the difference in the anchor density (Table
535 S2). β-glucan is known to form triple helix structure in an aqueous solution [36,37],

536 whereas our previous data using congo red suggested that introduction of MGlu units to
537 curdlan interfered the triple helix formation of curdlan derivatives [24]. Since both of
538 curdlan derivatives and Aquaβ derivatives used in this study might also take random
539 coil structure in an aqueous solution, an increase in the anchor density by introducing
540 anchor groups into branched monosaccharide units of Aquaβ would increase the
541 possibility of decyl group insertion into liposomal membrane *via* hydrophobic
542 interaction, resulting in efficient fixation of Aquaβ derivatives onto liposomes compared
543 with linear curdlan derivatives.

544 β-glucan derivatives induced secretion of inflammatory cytokines from DC2.4 cells.
545 Their modifications onto liposomes further increased the amounts of secreted cytokines,
546 even though the amounts of β-glucan derivatives added to the cells in later experiments
547 were rather low: the concentrations of β-glucan derivatives in Figs. 4a-b and 4c-d were
548 calculated as 0.5 mg/mL and 0.06–0.13 mg/mL, respectively. Modification of β-glucan
549 derivatives onto liposomes might exert a multivalent effect of β-glucan derivatives and
550 induce a strong activation signal *via* receptors on DCs [38]. When compared between
551 liposomes modified with an almost identical amount of curdlan derivatives or Aquaβ
552 derivatives (Fig. 4e), Aquaβ derivative-modified liposomes induced cytokine secretion
553 from DCs more effectively than curdlan derivative-modified liposomes did. The results

554 suggest that the backbone structure of β-glucan derivatives affects the adjuvant ability
555 of the β-glucan derivative-modified liposomes. Furthermore, high MGlu density of
556 Aquaβ derivative-modified liposomes derived from branching structure of Aquaβ might
557 also contribute the remarkable activation of DCs (Fig. S6). Liposomes modified with
558 Aquaβ derivatives with low MGlu% showed higher cellular association than that of
559 liposomes modified with curdlan derivatives with low MGlu% (Fig. 5a). This might
560 result from high MGlu density of Aquaβ derivative-modified liposomes compared with
561 curdlan derivative-modified liposomes. The results suggest that conventional curdlan
562 derivative-modified liposomes were taken up mainly *via* scavenger receptors (Fig. 5b),
563 which is consistent with our previous report using curdlan derivative-modified
564 liposomes [24]. The cellular uptake of Aquaβ derivative-modified liposomes was also
565 fundamentally inhibited by the addition of dextran sulfate, but the effect diminished as
566 the MGlu% of Aquaβ derivatives increased (Fig. 5b). Surprisingly, in MGlu70-Aquaβ-
567 A6-modified liposomes, the addition of dextran sulfate promoted intracellular uptake.
568 Taken together, the detailed mechanisms by which the cells recognize Aquaβ
569 derivatives remain elusive. Additional experiments using other inhibitors for Dectin-1
570 or TLRs, or knockout of these receptors are necessary to reveal interaction mechanisms
571 between Aquaβ derivatives and the cells.

572 In our previous report, administration of curdlan derivative-modified liposomes
573 induced significant suppression of tumor growth [24]. By contrast, in this study, OVA-
574 loaded, curdlan derivative-modified liposomes did not suppress tumor growth in some
575 mice (Fig. S7). We infer that this is true because we performed liposome administration
576 at a later stage of tumor growth (likely to be more immunosuppressive) than in
577 experiments in our previous report [24]. Average tumor volume at first injection in
578 current study was 324 ± 19.9 mm^3, which is 6.8-times larger than that of our previous
579 study (47.5 ± 10.8 mm^3). In such a later-stage tumor, antitumor immunity induced by
580 curdlan derivative-modified liposomes might not be sufficient to induce significant
581 tumor regression. Even in a late-stage tumor, administration of Aquaβ derivative-
582 modified liposomes significantly suppressed the growth of large E.G7-OVA tumors in
583 all mice compared with PBS and curdlan derivative-modified liposomes (Figs. 6 and
584 S7). After subcutaneous injection, Aquaβ derivative-modified liposomes that have high
585 modification efficiency of polysaccharide derivatives might be taken up by APCs and
586 promote inflammatory cytokine secretions from these cells, which resulted in effective
587 activation of antitumor cellular immune responses compared with curdlan derivative-
588 modified liposomes. $CD8^+$ T cells induced by immunization of Aquaβ derivative-
589 modified liposomes migrated to the tumor tissue effectively (Fig. 7b), which contributed

590 the significant suppression of tumor growth directly. Macrophages in a tumor are
591 polarized to tumor-suppressive M1-phenotype by stimulation with IFN-γ [39,40].
592 Consequently, IFN-γ secretion from $CD8^+$ T cells infiltrated to the tumor might also
593 induce the polarization of tumor-associated macrophages to M1-phenotyes and increase
594 M1/M2 ratio in the tumor (Figs. 8 and S10), which canceled immunosuppression within
595 tumor and assisted suppression of tumor growth in the treatment of Aquaβ derivative-
596 modified liposomes.

597

598 **5. Conclusion**

599 For this study, carboxylated Aquaβ derivatives, which has a branched structure as a
600 backbone, were synthesized to enhance the antitumor efficacy of antigen-loaded
601 liposomes. Modification efficiency of Aquaβ derivatives to the liposomes was
602 significantly higher than that of conventional curdlan derivatives. Aquaβ derivatives-
603 modified liposomes released their cargo in response to weakly acidic pH, which
604 corresponds to an endosomal/lysosomal environment. OVA-loaded, Aquaβ derivatives-
605 modified liposomes interacted effectively with a DC cell line and induced secretion of
606 inflammatory cytokines. Furthermore, the liposomes increased the percentage of

607 intratumoral $CD8^+$ T cells and polarized intratumoral macrophages to M1-phenotype,
608 resulting in significant growth suppression of large E.G7-OVA tumor in mice. Results
609 obtained from this study underscore the importance of the selection of backbone
610 structure to induce strong cellular immunity and to obtain the enhanced therapeutic
611 effects. The results demonstrate that Aquaβ derivative-modified liposomes can be
612 promising materials for liposomal vaccines to achieve efficient delivery of antigens,
613 activation of DCs and antigen-specific immunity.

614

615 **Acknowledgments**

616 This research was funded by Grants-in-aid for Scientific Research from the
617 Ministry of Education, Science, Sports, and Culture in Japan, grant number
618 (15H03024). The authors thank Takumi Tsujimura and Misaki Kitagawa (Osaka
619 Prefecture University) for their kind support on animal experiments. The authors
620 appreciate Dr. Maki Ohashi (Sanyo Fine Co., Ltd.) for his kind support on Aquaβ
621 providing.

622

623 **CRediT author statement**

Shin Yanagihara: Data curation, Formal analysis, Investigation, Methodology, Writing - original draft, **Nozomi Kasho**: Data curation, Formal analysis, Investigation, Methodology, **Koichi Sasaki**: Data curation, Formal analysis, Investigation, Methodology, Writing - original draft, **Naoto Shironaka**: Investigation, Methodology, **Yukiya Kitayama**: Data curation, Formal analysis, Writing - review & editing, **Eiji Yuba**: Conceptualization, Data curation, Formal analysis, Funding acquisition, Investigation, Methodology, Project administration, Supervision, Validation, Writing - original draft, Writing - review & editing, **Atsushi Harada**: Data curation, Formal analysis, Project administration, Supervision, Validation, Writing - review & editing.

References

1. S. Khan, D.E. Gerber, *Semin. Cancer Biol.*, 2020, **64**, 93-101.
2. R. Khazen, S. Müller, F. Lafouresse, S. Valitutti, S. Cussat-Blanc, *Sci. Rep.*, 2019, **9**, 1208.
3. N. Varadarajan, B. Julg, Y.J. Yamanaka, H. Chen, A.O. Ogunniyi, E. McAndrew, L.C. Porter, A. Piechocka-Trocha, B.J. Hill, D.C. Douek, F. Pereyra, B.D. Walker, J.C. Love, *J. Clin. Invest.*, 2011, **121**, 4322-4331.
4. S. Rosenberg, J. Yang, N. Restifo, *Nat Med*, 2004, **10**, 909–915.
5. N.I. Ho, L.G.M. Huis in 't Veld, T.K. Raaijmakers, G.J. Adema, *Front. Immunol.*, 2018, **9**, 2874.
6. A. Rodriguez, A. Regnault, M. Kleijmeer, P. Ricciardi-Castagnoli, S. Amigorena, *Nat. Cell Biol.*, 1999, **1**, 362–368.
7. O. Joffre, E. Segura, A. Savina, S. Amigorena, *Nat. Rev. Immunol.*, 2012, **12**, 557-569.
8. S. Burgdorf, A. Kautz, V. Bohnert, P.A. Knolle, C. Kurts, *Science*, 2007, **316**, 612-616.
9. A. Ahmad, J.M. Khan, S. Haque, *Biochimie*, 2019, **160**, 61-75.
10. J. Zepeda-Cervantes, J.O. Ramírez-Jarquín, L. Vaca, *Front. Immunol.*, 2020, **11**, 1100.
11. J. Sheen, M.G. Strainic, J. Liu, W. Zhang, Z. Yi, M.E. Medof, P.S. Heeger, *J. Immunol.*, 2017, **199**, 278-291.

12. S. Saijo, N. Fujikado, T. Furuta, S. Chung, H. Kotaki, K. Seki, K. Sudo, S. Akira, Y. Adachi, N. Ohno, T. Kinjo, K. Nakamura, K. Kawakami, Y. Iwakura, *Nat. Immunol.*, 2007, **8**, 39-46.
13. P.R. Taylor, D.M. Reid, S. Heinsbroek, G.D. Brown, S. Gordon, S. Wong, *Eur. J. Immunol.*, 2005, **35**, 2163-2174.
14. C. Zilker, D. Kozlova, V. Sokolova, H. Yan, M. Epple, K. Überla, V. Temchura, *Nanomedicine*, 2017, **13**, 173-182.
15. X. Dong, J. Liang, A. Yang, Z. Qian, D. Kong, F. Lv, *ACS Appl. Mater. Interfaces*, 2019, **11**, 4876-4888.
16. F. Aosai, M.S. Rodriguez Pena, H.S. Mun, H. Fang, T. Mitsunaga, K. Norose, H.K. Kang, Y.S. Bae, A. Yano, *Cell stress & chaperones*, 2006, **11**, 13–22.
17. J. Banchereau, R. Steinman, *Nature*, 1998, **392**, 245-252.
18. E. Yuba, C. Kojima, A. Harada, Tana, S. Watarai, K. Kono, *Biomaterials*, 2010, **31**, 943-951.
19. E. Yuba, A. Harada, Y. Sakanishi, K. Kono, *J. Controlled Release*, 2011, **149**, 72-80.
20. E. Yuba, N. Tajima, Y. Yoshizaki, A. Harada, H. Hayashi, K. Kono, *Biomaterials*, 2014, **35**, 3091-3101.
21. M. Okubo, M. Miyazaki, E. Yuba, A. Harada, *Bioconjugate Chem.*, 2019, **30**, 1518-1529.
22. S. Saijo, N. Fujikado, T. Furuta, S. Chung, H. Kotaki, K. Seki, K. Sudo, S. Akira, Y. Adachi, N. Ohno, T. Kinjo, K. Nakamura, K. Kawakami, Y. Iwakura, *Nat. Immunol.*, 2007, **8**, 39-46.
23. H.L. Rosenzweig, J.S. Clowers, G. Nunez, J.T. Rosenbaum, M.P. Davey, *Inflamm. Res.*, 2011, **60**, 705-714.

24. E. Yuba, A. Yamaguchi, Y. Yoshizaki, A. Harada, K. Kono, *Biomaterials*, 2017, **120**, 32-45.
25. H. Kono, N. Kondo, K. Hirabayashi, M. Ogata, K. Totani, S. Ikematsu, M. Osada, *Carbohydr. Polym.*, 2017, **174**, 876-886.
26. D. Muramatsu, K. Kawata, S. Aoki, H. Uchiyama, M. Okabe, T. Miyazaki, H. Kida, A. Iwai, *Sci. Rep.*, 2014, **4**, 777.
27. D. Fujikura, D. Muramatsu, K. Toyamane, K. Toyomae, S. Chiba, T. Daito, A. Iwai, T. Kouwaki, M. Okamoto, H. Higashi, H. Kida, H. Oshiumi, *J. Biochem.*, 2018, **163**, 31-38.
28. Y. Kimura, M. Sumiyoshi, T. Suzuki, T. Suzuki, M. Sakanaka, *Int. Immunopharmacol.*, 2007, **7**, 963-972.
29. I. Popescu, I.M. Pelin, G.L. Ailiesei, D.L. Ichim, D.M. Suflet, *Carbohydr. Polym.*, 2019, **224**, 115157.
30. S.S. Nielsen (Ed.), *Food Analysis Laboratory Manual. Food Science Text Series, Springer, Cham (2017)*, 2017, 137-142.
31. T. Masuko, A. Minami, N. Iwasaki, T. Majima, S. Nishimura, Y. C. Lee, *Anal. Biochem.*, 2005, **339**, 69-72.
32. Y. Yoshizaki, E. Yuba, N. Sakaguchi, K. Koiwai, A. Harada, K. Kono, *Biomaterials*, 2017, **141**, 272-283.
33. N. Platt, H. Suzuki, Y. Kurihara, T. Kodama, S. Gordon, *Proc. Natl. Acad. Sci. U.S.A.*, 1996, **93**, 12456-12460.
34. M.A. Aghdam, R. Bagheri, J. Mosafer, B. Baradaran, M. Hashemzaei, A. Baghbanzadeh, M. de la Guardia, A. Mokhtarzadeh, *J. Controlled Release*, 2019, **315**, 1-22.

35. E. Yuba, *J. Mater. Chem. B*, 2020, **8**, 1093.
36. K. Miyoshi, K. Uezu, K. Sakurai, S. Shinkai, *Chem. Biodivers.*, 2004, **1**, 916-924.
37. H. Kono, N. Kondo, T. Isono, M. Ogata, K. Hirabayashi, *Int. J. Biol. Macromol.*, 2020, **154**, 1382-1391.
38. H. Duan, M. Donovan, A. Foucher, X. Schultze, S. Lecommandoux, *Sci. Rep.*, 2018, **8**, 14730.
39. R.D. Stout, C. Jiang, B. Matta, I. Tietzel, S.K. Watkins, J. Suttles, *J. Immunol.*, 2005, **175**, 342-349.
40. K.J. Mylonas, M.G. Nair, L. Prieto-Lafuente, D. Paape, J.E. Allen, *J. Immunol.*, 2009, **182**, 3084-3094.